



AN INTEGRATIVE *IN SILICO* CHARACTERIZATION AND DOCKING STUDIES OF
 β - ENOLASE: A NOVEL THERAPEUTIC INSIGHT FOR
 β - -ENOLASE DEFICIENCY



Corresponding Author

SINOSH SKARIYACHAN

Department of Biotechnology, Dayananda Sagar College of
Engineering, Bangalore, Karnataka, India

Co Authors

NARASIMHA SHARMA AND ARPITHA B M

Department of Biotechnology, Dayananda Sagar College of Engineering, Bangalore, Karnataka, India

ABSTRACT

The β -Enolase protein deficiency causes the glycogen storage disease type 13- β -Enolase deficiency. An *in silico* comparative modelling and docking studies were conducted as the structural information about the protein was unavailable in any of the structural databases. The crystal structure of neuron specific enolase (PDBID: 1TE6, Chain A) was selected as best template and it was modelled by MODELLER 9v7. The PROCHECK analysis accounted for 92% of the residues in the most favored region of Ramachandran plot and structure quality factor is 95.30%. The protein showed 0.1 Å RMSD and it is submitted to Protein Model Database with ID: PM0076547. The docking studies with selected ligands were conducted and concluded that Nonaethylene glycol was the best ligand of choice with $E_{\text{total}} = -95.82$. Hence, with the reliable β -Enolase Protein model and the docking studies, it infers that this inhibitor can be used as a potential drug candidate against β -Enolase protein.

This article can be downloaded from www.ijpbs.net



KEYWORDS

β -Enolase, *In silico* Modelling, MODELLER 9v7, Molecular docking, Nonaethylene Glycol.

INTRODUCTION

Enolase (EC 4.2.1.11) is an enzyme catalyzing the reversible conversion of 2-phosphoglycerate into phosphoenolpyruvate in the presence of Mg^{2+} ions. Enolase in crystalline form was obtained for the first time from human muscles by Baranowski and coworkers in 1968 in the Department of Medical Biochemistry, Wrocław Medical University^{1,2}.

The enzyme can be found from Archaeobacteria to mammals, and is a member of a large super family comprising among other carboxy phosphoenolpyruvate synthase^{3,4}. In vertebrates three tissue-specific isoenzymes were identified: non-neuronal enolase (NNE, α), neuron-specific enolase (NSE, γ) and muscle-specific enolase (MSE, β)⁵. Each isoform is encoded by a distinct gene whose expression is regulated in a tissue-specific and development-specific manner^{6,7,8,9}. Biochemical research of enolases has practical applications in cancer and allergy diagnostics¹⁰. ENO3 is a muscle specific form of enolase, associated with glycolysis and inherited recessive metabolic myopathy in

humans. The decreased expression of ENO3 may be associated with its role in glycolysis, and potentially suggests a reduced requirement for energy in the differentiating skin¹¹. Several proteins functioning in the glycolytic pathway were differentially expressed, including enolase and GAPDH. Enolase is the enzyme catalyzing the ninth step of glycolysis, the mechanism involves the transfer of a phosphoryl group from phosphoenolpyruvate which are formed by the actions of enolase in the glycolysis^{12,13}.

Since the number of possible folds in nature appears to be limited¹⁴ and the 3D structure of proteins is better conserved than their sequences, it is often possible to identify a homologous protein with a known structure (template) for a given protein sequence (target). Homology modelling has proven to be the method of choice to generate a reliable 3D model of a protein from its amino acid sequence.^{15,16}

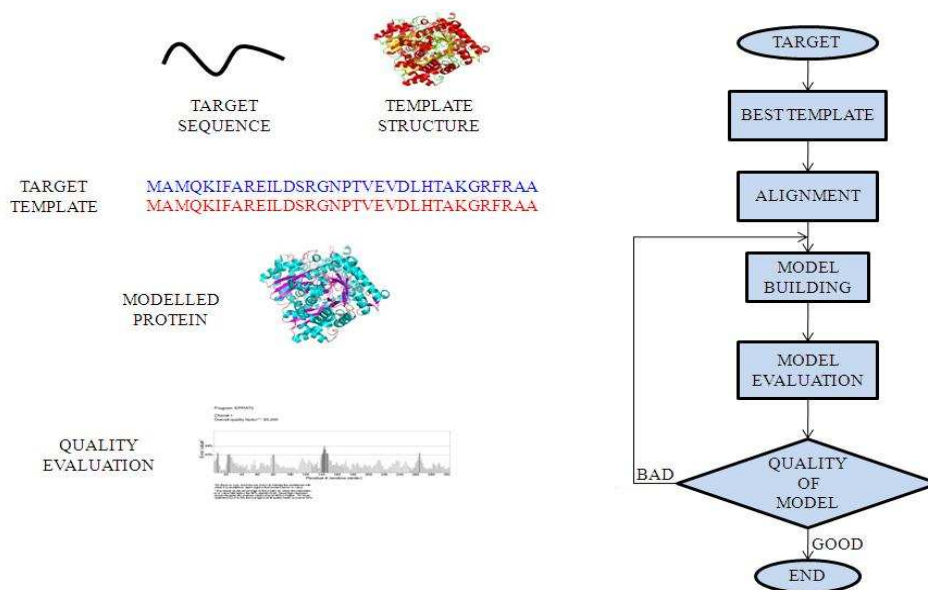


Fig1
Steps involved in the homology modelling of β -enolase

Homology modelling of the β -Enolase protein was conducted by Modeller 9v7. MODELLER implements comparative protein structure modelling (Fig 1) by satisfaction of spatial restraints that include (i) homology-derived restraints on the distances and dihedral angles in the target sequence, extracted from its alignment with the template structures¹⁷, (ii) stereochemical restraints such as bond length and bond angle preferences, obtained from the CHARMM-22 molecular mechanics force-field¹⁸, and (iii) statistical preferences for dihedral angles and non-bonded inter-atomic distances, obtained from a representative set of known protein structures^{19, 20}.

Predicting interactions between small molecules and proteins is a key element in the drug discovery process. In particular, several classes of proteins such as G-protein-coupled receptors, enzymes and ion channels represent a large fraction of current drug targets and important targets for new drug development²¹.

This study was conducted using Hex 6.1²², it uses Spherical Polar Fourier (SPF) correlations to calculate the docking scores.

MATERIALS AND METHODS

Retrieval of β -Enolase Protein Sequence and Selection of the Best Homolog from RCSB-PDB

The β -Enolase protein sequence (UniProt ID: P13929) was retrieved in the FASTA Format and submitted to PSI-BLAST for getting the best structural homologs of the β -Enolase protein. The sequence data of the best homologs were subjected to Multiple Sequence Alignment and Phylogenetic Characterization. MSA was performed by T-COFFEE²³ to analyze the conservation factor in the closely related proteins. The guide tree created from the best homologs of the β -Enolase protein was submitted to TreeView to



view the phylogenetic evolutionary pattern of the homolog set. The closest protein to β -Enolase was selected as the best template and its structure was retrieved from RCSB-PDB.

Proteogenomic Characterization of β -Enolase Protein

The β -Enolase protein sequence was reverse translated by the Reverse Translate tool hosted in the ExPASy server. The nucleotide sequence of β -Enolase was subjected to Open Reading Frame analysis by the NCBI-ORF Finder. The locations of the Functional genes present in the nucleotide sequence of β -Enolase were analyzed by the GENSCAN²⁴.

The Secondary structure conformations of the β -Enolase protein sequence were predicted by PSIPRED²⁵. The Hydrophobicity Profile of the β -Enolase protein was generated by TopPred²⁶. The Functional Motifs in the β -Enolase protein sequence was found by the SMART²⁷ tool. The Post Translational Modifications present in the β -Enolase protein sequence were predicted by dbPTM²⁸.

In silico Comparative Modelling of the β -Enolase Protein

An *in silico* comparative modelling of the β -Enolase Protein was performed by the MODELLER 9v7²⁹. The best homolog identified earlier in the proteogenomic characterization was used to generate alignment, atom and the script files for modelling. The target and template were superimposed by DaliLite³¹ server to analyze the RMSD value. The Modelled β -Enolase Protein was visualized by PyMOL³⁰.

Model refinement, validation and Submission of modelled β -Enolase protein to PMDB

The modelled protein is validated by various molecular dynamics and mechanics with the help of various empirical force fields such as

ANNOLEA³², GROMOS³³ and VERIFY3D³⁴. The parameters included the covalent bond distances and angles, stereochemical validation and atom nomenclature were validated using PROCHECK³⁵. The statistics of non-bonded interactions between different atom types was detected and value of the error function was analyzed by ERRAT³⁶. The modelled β -Enolase Protein was deposited to the Protein Model Data Bank.

Selection of Potential Drug Candidates against β -Enolase protein

On the basis of extensive literature studies and drug database survey, about 10 inhibitors were selected for docking process to identify the potential drug candidate against the β -Enolase protein related disorders. The selected inhibitors are Nonaethylene Glycol³⁷, Telenzepine dihydrochloride³⁸, Flouride³⁹, Phosphonoacetohydroxamate⁴⁰, Creatine⁴¹, Biocytin⁴², Glycine methyl ester⁴³, 2-Phosphoglycerate^{44, 45}, Glyceraldehyde-3-phosphate⁴⁶, Trihydroxyheptanoic acid and 2-Aminoethyl-methanesulfonate. The structural coordinates of these molecules were retrieved from NCBI PubChem⁴⁷ in SDF format and converted to PDB format using OpenBabel 2.2.3.

Molecular Docking

A rigid body docking was performed with HEX 6.1⁴⁸ by SP Fourier Transform, FFT steric Scan, FFT final Search and MM refinement. The clustering histogram with the scoring function was generated to analyze the binding energy of each selected conformations. The energy values in the clustering histogram of the docked complexes were analyzed. The ligand that produced the best E_{Total} , minimum energy, was selected as the best inhibitor against β -Enolase Protein. The docked complex was



viewed and the interaction residues of amino acids with the ligands were analyzed by PyMOL

RESULTS AND DISCUSSION

Retrieval of β -Enolase Protein Sequence and Selection of the Best Homologs from RCSB-PDB

The β -Enolase protein sequence retrieved from Uniprot (ID: P13929) consists of 434 amino acids. The major functionalities of the β -Enolase protein are, it plays a major role in striated muscle development and regeneration and also in glycolysis process as a catalyst for the interconversion of 2-phospho-D-glycerate and phosphoenolpyruvate. The FASTA format of β -Enolase was accessed from the Flat file and the

PSI – BLAST results represented the proteins with high homology with the β -Enolase protein. FASTA sequences of the best ten templates were retrieved from NCBI. The identity range was 63-83%, similarity range was 92-79% and E- value range was 0 to $1e-161$. The T-COFFEE server successfully displayed the MSA and the clustering phylogram was opened using TreeView program. (Fig. 2). The evolutionary studies with phylogram showed the crystal structure of human neuron specific enolase, 1.8 \AA (PDB ID: 1TE6, Chain A) could be used as the suitable template for modelling. The template protein consists of 449 amino acids in Chain A and it consists of 43% helical structures and 17% beta sheet.

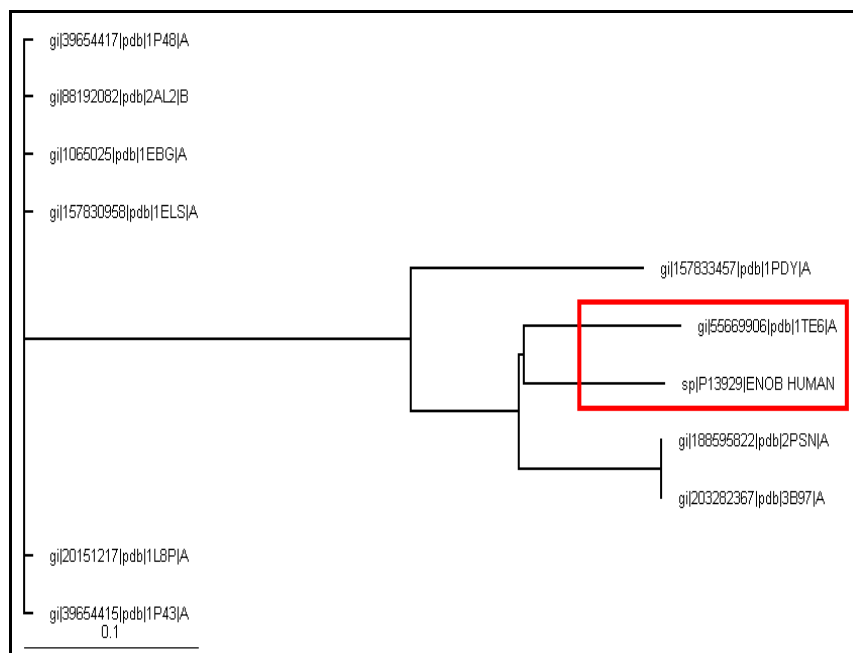


Fig 2
Phylogenetic Characterization of the best homologs of β -Enolase



Proteogenomic characterization of β -Enolase Protein

The Reverse Translate tool predicted the β -Enolase protein to have 1302 nucleotide bases in the sequence. The ORF Finder displayed the possible six frames of translation of the reverse translated β -Enolase protein sequence. Out of the 6 possible frames of translation only the +1, +2, -1, -2, and -3 Frame possess the potential to translate to protein sequences. The +1 Frame was the longest coding 1302 nucleotides. GENSCAN also predicted different variables of functional sites in the nucleotide sequence.

The secondary structures prediction of β -Enolase indicated that it consists of majority of helices of about 43.32% and random coils about 33.18% extended strands of about 15.67% and beta turns of about 7.83%. On basis of these results it was interpreted that β -Enolase protein consists of alpha helical structure. The TopPred analysis interpreted the Hydrophobicity and Topology of β -Enolase protein. The Hydrophobicity of the protein varies extensively between -4 and +1. The upper cut off range was at +1 and the lower cut off range was at +0.75. The topology results indicated that the loop length of the protein varied from 103 to 310. The

major domains present in the protein was predicted by SMART and it has two domains, Enolase_N and Enolase_C domains consisting Pfam ID: PF03952 and PF00113 respectively. Enolase_N domain ranges from 2 to 134 amino acids, Enolase_C domain ranges from 142 to 432. The low complexity region is identified between 216 and 227 amino acids. The dbPTM predicted major Post Translational Modifications, protein variants and the secondary structures. About five types of PTMs were predicted including N-linked Asparagine, O-linked Serine, Phosphotyrosine, Phosphoserine and Methyl lysine.

In silico Comparative Modelling of the β -Enolase Protein

The sequence information of human neuron specific enolase was described in the materials and methods. The pair wise alignment between target and template was performed (Fig.3). The superimposition with DaliLite was performed to analyze the backbone threading of template and target. (Fig.4). It has been noticed that RMSD value is 0.1 which indicates the backbone configuration of the protein is perfect.



Fig 3
Sequence alignment between target Enolase and template

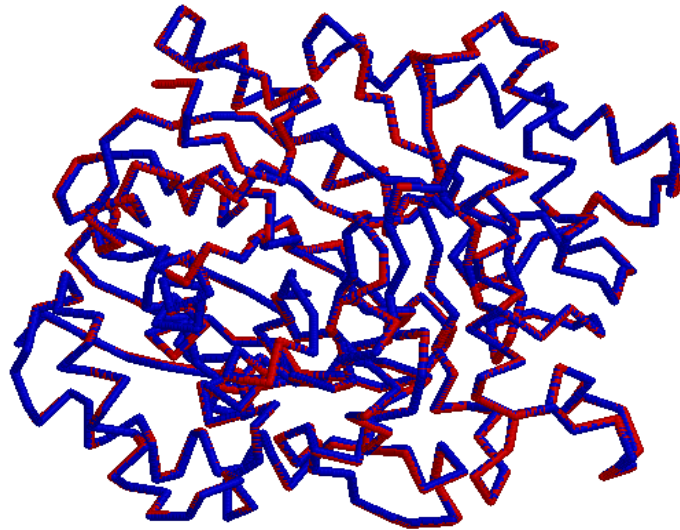


Fig 4

The target protein of Enolase is threaded against template structure

Secondary structure assessment by STRIDE provided physical skeleton of modelled proteins such as helices, extended strand and coil. Our modelled protein primarily consists

more of alpha helices and random coil than extended strand. The 3D generated model was displayed by PyMol for visual interpretation (Fig.5).

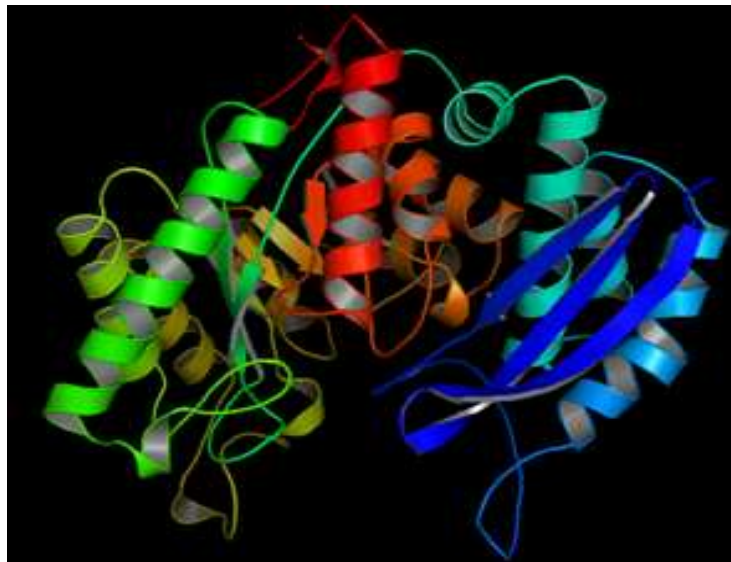


Fig5

Modelled structure of β -Enolase Protein

This article can be downloaded from www.ijpbs.net

Refinement and validation of modelled β -Enolase

The refinement of model was done by various empirical force fields such as ANOLEA, GROMOS and VERIFY-3D. The modelled protein is validated by Ramachandran Plot generated by PROCHECK. The Ramachandran Plot results read as 92% of the residues in the most favored regions, 7.5% of the residues in the additionally

allowed regions, about 0.3% in the generously allowed and disallowed regions each (Fig.6). The ERRAT value inferred the overall quality factor of the model as 95.305 %. The Z score values read as the Z score mean: 0.519, Z score standard deviation: 23.46 and Z scores RMS: 23.46. All these results concluded that the model was of good quality.

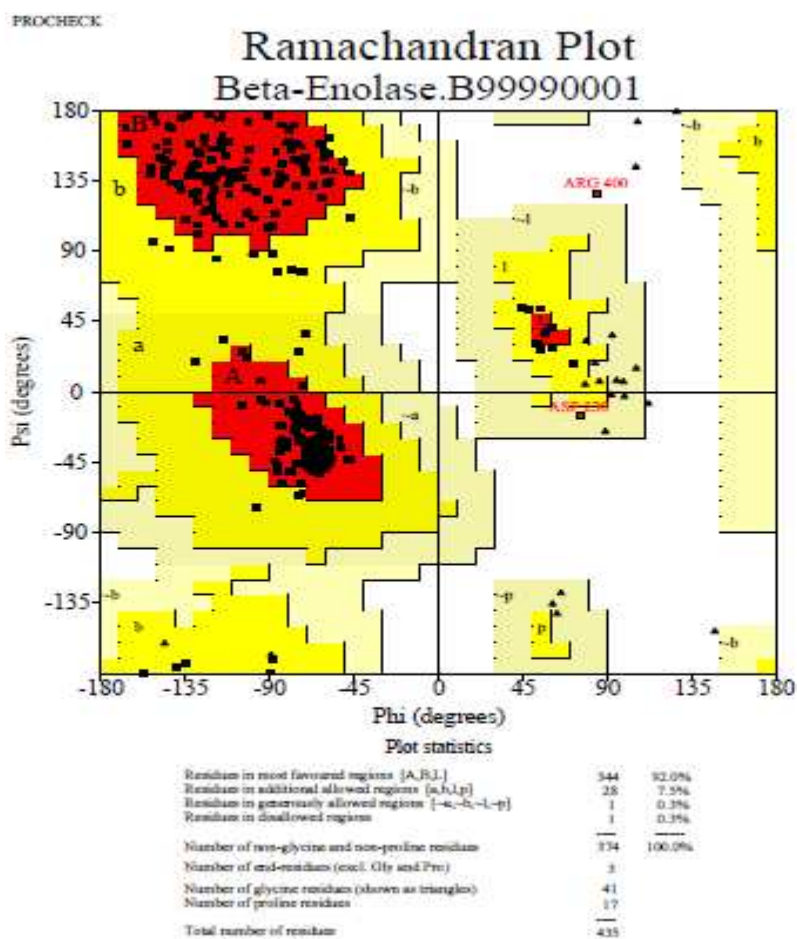


Fig 6
 Ramachandran plot of Modelled protein generated by PROCHECK

Submission of Modelled structure to Protein Modelling Database

The modelled structure of β -Enolase was submitted to the Protein Model Data Bank. PMDB ID: PM0076547 was obtained for the β -Enolase protein model and can be downloaded for further studies.

Molecular Docking studies

Nonaethylene Glycol is the best inhibitor to be identified in our study, the clustering histogram of docked complex given a minimum energy score of -95.82 which shows better binding than other inhibitors (Table 1). The important residues interacting with Nonaethylene Glycol are ARG 132, PRO 141, ASP 142, LYS 420, ALA 421, ALE 422, LYS 432, ALA 433 and LYS 434 which forms strong bond with the receptor (Fig. 7)

Table 1
Docking binding energies of selected inhibitors against modelled enolase

Si No.	PubChem ID	COMPOUND	ENERGIES
1	CID: 11339376	Nonaethylene Glycol	-95.8
2	CID: 6419995	Telenzepine dihydrochloride	-57
3	CID: 44291436	Flouride	-56.5
4	CID: 11969443	Phosphonoacetohydroxamate	-38.2
5	CID: 586	Creatine	-36
6	CID: 83814	Biocytin	-34.1
7	CID: 69221	Glycine methyl ester	-31.6
8	CID: 11708158	Trihydroxyheptanoic acid	-31.5
9	CID: 11579140	2-Aminoethyl-methanesulfonate	-28.3
10	CID: 59	2-Phosphoglycerate	-23.2
11	CID: 729	Glyceraldehyde 3-phosphate	-18.1

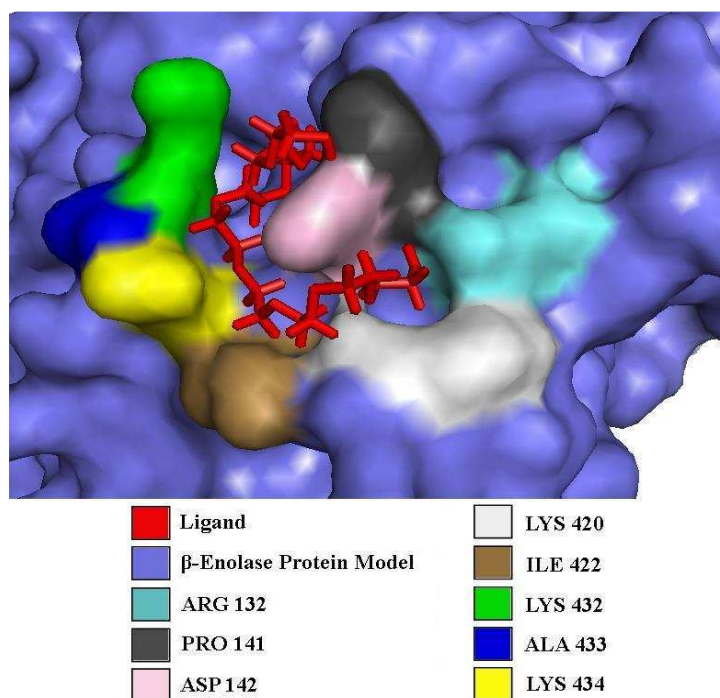


Fig 7
Interaction of modelled protein with Nonaethylene Glycol

CONCLUSION

β -Enolase protein plays a major role and also acts as marker in many disorders such as Rhabdomyosarcoma, Muscular Dystrophy, Glycogen Storage disease, Congenital Dystrophy, Epistaxis, Osteosarcoma, Malaria, Acute Myocardial Infarction, Pneumoniae etc., The important mechanism in treating any disease is targeting the malfunctioning protein structure with suitable ligands also known as potential drug candidates. The 3D protein structure must be known in this case to achieve the above foresaid. As no X-ray crystallographic or NMR structures of β -Enolase protein were reported in any of the structural databases an *in silico* study was significant.

The β -Enolase protein sequence was retrieved from Uniprot and PSI-BLAST search was performed to obtain the best and the nearest homologs of β -Enolase. The crystal structure PDB ID: 1TE6, Chain A was selected as the template for modelling the protein with MODELLER 9v7. The β -Enolase protein was then subjected to various kinds of validation and refinement techniques. The PROCHECK analysis resulting 92% of the residues of the protein in the most favoured regions in the Ramachandran Plot, the model quality factor was 95.305 and RMSD value reporting to be 0.1, it was interpreted that the modelled structure of β -Enolase was of excellent quality. The suitable ligands against the β -Enolase protein were shortlisted based on the survey of various literatures. The ligands were obtained from PubChem and docked against the



modelled protein to select the best. Out of the 10 docked ligands, Nonaethylene Glycol was found to be the best ligand which returned an E value of -95.82 in the clustering histogram and has maximum number of interacting residue with the protein. Hence our study concluded that the modelled protein was of high quality and Nonaethylene Glycol could be acted as a potential drug candidate against β -Enolase protein.

REFERENCES

1. Baranowski T and Wolna E, Enolase from human muscle, *Methods Enzymol*, 42: 335–338. (1975).
2. Baranowski T, Wolna E, Morawiecki A, Purification and properties of crystalline 2-phospho-glycerate hydro-lyase from human muscle, *Eur J Biochem*, 5: 119–123.(1968)
3. Pegg S.C and Babbit P.C, Shotgun: getting more from sequence similarity searches, *Bioinformatics* 15: 729–740. (1999)
4. Babbit P.C, Hasson M.S, Wedekind J.E, Palmer D.R, Barre W.C, Reed G.H, Rayment I, Ringe D, Kenyon G.I, Gerlt J.A, The enolase superfamily: a general strategy for enzyme-catalyzed abstraction of the alpha-protons of carboxylic acids, *Biochemistry*, 35: 16489–16501. (1996).
5. Rider C.C and Taylor C.B, Enolase isoenzymes. II. Hybridization studies developmental and phylogenetic aspects, *Biochim Biophys Acta* 405: 175–187. (1975)
6. Giallongo A, S. Venturella, D. Oliva, G. Barbieri, P. Rubino, S. Feo, Structural features of the human gene for muscle specific enolase: differential splicing in the 59 untranslated sequence generates two forms of mRNA, *Eur. J. Biochem.* 214:367–374. (1993).
7. Oliva D, L. Cali, S. Feo, A. Giallongo, (1991), Complete structure of the human gene encoding neuron-specific enolase, *Genomics* 10:157–165. (1991).
8. Feo S, D. Oliva, G Barbieri, W. Xu, M. Fried, A. Giallongo, The gene for the muscle-specific enolase is on the short arm of human chromosome 17, *Genomics* 6:192–194. (1990).
9. Giallongo A. D, Oliva, L. Cali, G. Barba, G. Barbieri, S. Feo, Structure of the human gene for alpha enolase, *Eur. J. Biochem*, 190:567– 573. (1990)
10. Nitter-Marszalska M, Kustrzeba-Wójcicka I, Pisarczyk-Bogacka E, Medrala W, Patkowski J, Skin test with enolase in the diagnosis of fungal allergy, *Allergy* 53: 30. (1998)
11. Comi G.P, Fortunato F., Lucchiari S, Bordoni A, Prella A, Jann S, Keller A, Ciscato P, Galbiati S, Chiveri L, Torrente Y, Scarlato G, Bresolin N, Beta enolase efficiency, a new metabolic myopathy of distal glycolysis, *Ann. Neurol.* 50 202–207. (2001)
12. Sanchez B, Champomier-Verges M.C, Stuer-Lauridsen B, Ruas-Madiedo P, Anglade P, Baraige F, de los Reyes-Gavilan C.G, Johansen E, Zagorec M, Margolles A, Adaptation and response of *Bifidobacterium animalis* subsp. *lactis* to

ACKNOWLEDGMENT

The authors would like to acknowledge the support and facilities provided by the R & D Centre, Department of Life Sciences and Engineering, Dayananda Sagar Institutions, Shavige Malleswara Hills, Kumaraswamy Layout, Bangalore, Karnataka, India



- bile: a proteomic and physiological approach. *Appl Environ Microbiol*, 73:6757-6767. (2007)
13. Sanchez B, Champomier-Verges M.C, Anglade P, Baraige F, de Los Reyes- Gavilan C.G, Margolles A, Zagorec M, Proteomic analysis of global changes in protein expression during bile salt exposure of *Bifidobacterium longum* NCIMB 8809. *J Bacteriol*, 187:5799-5808(2005).
 14. Chothia C, Proteins. One thousand families for the molecular biologist, *Nature*, 357, 543–544. (1992)
 15. Moult J, A decade of CASP: progress, bottlenecks and prognosis in protein structure prediction, *Curr Opin Struct Biol.*, 15, 285–289. (2005).
 16. Tramontano A and Morea V, Assessment of homology-based predictions in CASP5. *Proteins*, 53:352–368. (2003).
 17. Sali and Blundell, Comparative protein modelling by satisfaction of spatial restraints, *J. Mol. Biol.* 234, 779–815. (1993).
 18. MacKerell A. D, Jr Bashford D, Bellott M, Dunbrack R. L, Jr Evanseck, J. D. Field, M. J, Fischer S, Gao J, et al., All-atom empirical potential for molecular modelling and dynamics studies of proteins, *J.Phys.Chem.B.* 102, 3586-3616. (1998).
 19. Shen M. Y, and Sali A, Statistical potential for assessment and prediction of protein structures, *Protein Sci.* 15, 2507-2524. (2006).
 20. Sali A, and Overington J. P, Derivation of rules for comparative protein modelling from a database of protein structure alignments, *Protein Sci* 3, 1582-1596. (1994)
 21. Hopkins A.L. and Groom C.R, The druggable genome, *Nat Rev Drug Discov*, 1, 727–730. (2002)
 22. Alex Mathew and Nixon Raj, Proceedings of the International Multi Conference of Engineers and Computer Scientists, Vol I, IMECS. (2009),
 23. T-Coffee: A novel method for multiple sequence alignments" C. Notredame, D. Higgins, *J. Heringa .J of Mol Bio*, 302, 205-217, (2000)
 24. Burge, C. and Karlin, S. Prediction of complete gene structures in human genomic DNA. *J. Mol. Biol.* 268, 78-94. (1997)
 25. McGuffin LJ, Bryson K, Jones. The PSIPRED protein structure prediction server. *Bioinformatics.* 16(4):404-5. (2000).
 26. Claros MG, von Heijne G. TopPred II: Improved software for membrane protein structure predictions. *Comput Appl Biosci.* 10:685-6. (1994)
 27. Jörg Schultz, Frank Milpetz, Peer Bork, Chris P. Ponting SMART, a simple modular architecture research tool: Identification of signaling domains. *Proc. Natl. Acad. Sci.* 95:5857-5864 (1998)
 28. Tzong-Yi Lee^{1,5}, Justin Bo-Kai Hsu¹, Wen-Chi Chang^{1,6}, Ting-Yuan Wang¹, Po-Chiang Hsu² and Hsien-Da Huang *BMC Res J.*2:111(2009).
 29. Sali A, Marti-Renom M A, Stuart A C, Fiser A, Sanchez R, Melo F, Comparative protein structure modeling of genes and genomes. *Annu Rev Biophys Biomol Struct* 29: 291-325. (2000).
 30. Daniel Seeliger and Bert L. de Groot Ligand docking and binding site analysis with PyMOL and Autodock/Vina, *J Comput Aided Mol Des.*24 (5): 417–422 (2010).
 31. L. Holm, S. Kääriäinen, P. Rosenström, and A. Schenkel, Searching protein structure databases with DaliLite v.3, *Bioinformatics*; 24(23): 2780–2781(2008).
 32. Melo F, Devos D, Depiereux E, Feytmans E. ANOLEA: a www server to assess protein structures. *Proc Int Conf Intell Syst Mol Biol.*5:187-90. (1997).



33. Cao Z, Lin Z, Wang J, Liu H. Refining the description of peptide backbone conformations improves protein simulations using the GROMOS 53A6 force field. *J Comput Chem.* 31(1):1-23(2009).
34. Eisenberg D, Lüthy R, Bowie JU, VERIFY3D: assessment of protein models with three-dimensional profiles. *Methods Enzymol.* 277:396-404. (1997).
35. Laskowski, R.A. PROCHECK: a program to check the stereochemical quality of protein structures. *J. Appl. Cryst.*, 26:283–291.(1993).
36. Colovos C, Yeates TO. Verification of protein structures: patterns of nonbonded atomic interactions. *Protein Sci:*1511-9.(1993)
37. Ehinger S, Schubert W.D, Bergmann S, Hammerschmidt S, Heinz D.W, Plasmin(ogen)-binding alpha-enolase from *Streptococcus pneumoniae*: crystal structure and evaluation of plasmin(ogen)-binding sites. *J Mol Biol* ; 343 :997-1005. (2004)
38. Anthony Altar C, Marquis P Vawter, Stephen D Ginsberg, Target Identification for CNS Diseases by Transcriptional Profiling, *Neuropsychopharmacology*, 34(1), 18–54. (2009)
39. Qin J, Chai G, Brewer J.M, Lovelace L.L, Lebioda L; Fluoride inhibition of enolase: crystal structure and thermodynamics. *Biochemistry* 45:793-800. (2006)
40. Ceri E. Pugh, Alexander B. Roy, Tim Hawkest, John L. Harwood, A new pathway for the synthesis of the plant sulpholipid, sulphoquinovosyl diacyl glycerol *Biochem J*, 309, 513-519. (1995).
41. Arrio-Dupont M, Foucault G, Vacher M, Douhou A, Cribier S, Mobility of creatine phosphokinase and beta-enolase in cultured muscle cells, *Biophys J*, 73 :2667-73. (1997)
42. Shayan H and Murphy T.H, 89(1): Restriction of peroxidase-mediated antibody reactivity to single neurons by local hydrogen peroxide production; *Neuroscience* 279-90. (1999)
43. Russell G.A and Fothergill L.A, Inactivation of chicken muscle enolase by carbodiimide and glycine methyl ester; *FEBS Lett*, 143:211-2. (1982).
44. Chung S, Arrell D.K, Faustino R.S, Terzic A, Dzeja P.P, Glycolytic network restructuring integral to the energetics of embryonic stem cell cardiac differentiation, *J Mol Cell Cardiol*, 48:725-34. (2010)
45. Toscano A and Musumeci O, Tarui disease and distal glycogenoses: clinical and genetic update; *Acta Myol*; 26: 105-7. (2007)
46. Wang Y, Bolton E, Dracheva S, Karapetyan K, Shoemaker BA, Suzek TO, Wang J, Xiao J, Zhang J, Bryant S H. An overview of the PubChem BioAssay resource. *Nucleic Acids Res:* 255-66 (2010).
47. Ritchie D W, Evaluation of protein docking predictions using Hex 3.1 in CAPRI rounds 1 and 2, *Proteins.* 98-106 (2003);